EXTENSIVE QUALITY CONTROL SEQUENCE FOR NON-DESTRUCTIVE CHARACTERIZATION OF IMPLANTS FOR DENTAL RESTORATIONS

Aura-Cătălina MOCANU[1,2], Adelina Florina DOBRE[1], Cătălina-Andreea DASCĂLU[1,2], Andreea MAIDANIUC[2*], Adrian ERNUȚEANU[2], Marian SOARE[2], Raluca ZAMFIR[1], Dan GHEORGHE[1], Adriana SACELEANU[3], Vicenţiu SACELEANU[3]

This paper presents the results of a quality control sequence applied for evaluating different commercial dental implants. Selected rootform dental implants were non-destructively tested by radiographic examination, for defects identification and by X-ray fluorescence spectroscopy, for positive material identification. The geometrical features of implants threads (pitch, width, depth, flank and angle) were compared using the results provided by macroscopical analysis. The differences in implants morphology and surface roughness (provided by the different surface treatments: machining, abrasive blasting, acid etching and anodization) were evaluated based on scanning electron microscopy results, which were subjected to image colorization, 3D reconstruction and calculation of 2D roughness parameters (R_a, R_z and R_t) using a dedicated software.

Keywords: dental implants, implant macrodesign, implant microdesign, nondestructive testing, radiographic examination, surface roughness, thread geometry.

1. Introduction

The global dental implants market is expected to be USD 6.81 billion by 2024, with main causes of dental injuries being road accidents and sport injuries [1]. This market is currently dominated by commercially pure titanium (cp-Ti) and titanium alloy (Ti6Al4V) implants, which are selected as biomaterials due to their corrosion resistance, passivation capacity and biocompatibility [2, 3].

A dental implant is a medical device inserted in the jawbone, or in close vicinity of the jawbone, in order to restore the loss of a dental function. The dental implants used in current practice are designed differently based on their *placement*

[1] Metallic Materials Science, Physical Metallurgy Department, Faculty of Materials Science and Engineering, University POLITEHNICA of Bucharest, Romania
[2] S.C. Nuclear NDT Research & Services S.R.L, Bucharest, Romania
[3] Faculty of Medicine, University *Lucian Blaga* Sibiu, Romania
- corresponding author: andreea.maidaniuc@nuclearndt.ro

(endosteal, subperiosteal, transosteal or intramucosal) and *geometry* (cylinder, thread, plateau, perforated solid, or vented). Also, dental implants are manufactured from different *material types* (metallic, ceramic/ceramic coated, polymeric or carbon compound-based), can be subjected to various *surface modifications* (for preparing smooth, machined, textured or coated surfaces) and have different *attachment mechanisms* (osseointegration or fibrointegration).

Implant failure has become increasingly important research area for many clinical areas [4-6]. Predictors for implant success and failure are generally divided into patient-related factors, implant characteristics, implantation area, and clinician experience [4]. In order to avoid implant failure, various quality control measures are adopted by implant manufacturers for guaranteeing that all design and material specifications are met [5]. While destructive material testing, such as chemical composition analyses, microstructure evaluation or mechanical testing are performed on sampled batches with representative products, the design and manufacturing flaws can be assessed for 100% of production lots by means of non-destructive testing.

A common non-destructive method used for metallic products is radiographic examination (RT); this has previously been employed in the quality control of dental products for evaluating porosities or for measuring occlusal thickness in medical castings manufactured from titanium [7], cobalt-chromium alloys [8] or precious metals [9]. Material grade can also be verified by means of non-destructive testing, using portable X-ray fluorescence spectrometers (XRF). For titanium and titanium alloys, many currently available portable XRF equipment can distinguish between Cp-Ti and Ti6Al4V, the most popular titanium alloy used in dental implants [10].

Given that the clinical success of a dental implant is closely correlated with its early osseointegration (i.e. direct bone-implant bonding, without an intermediate tissue), geometry and surface topography are key-parameters which influence both the short-term and long-term interaction between the implant and the biological environment [11-15]. A practical and non-destructive method for evaluating these parameters is scanning electron microscopy (SEM). Due to recent developments in digital image processing, SEM users can evaluate quantitative parameters related to thread geometry and surface roughness solely by analysing micrographs with dedicated software.

This paper presents the results of a quality control sequence based on non-destructive testing methods applied for evaluating different commercial dental implants. The purpose was to evaluate both the implants macrodesign (material, body shape, and thread geometry) and the microdesign (morphology and surface roughness) in a standardized and reproductible manner. Selected rootform dental implants were non-destructively tested for defects identification and positive material identification. Next, the geometrical features of implants threads (pitch,

width, depth, and angle) were compared starting from the results provided by macroscopical analysis, which were processed using a dedicated software for measuring the geometrical parameters. Implants morphology and the surface roughness (calculated based on image analysis performed on micrographs) were used for comparing the outcomes of the different surface treatments: machining, abrasive blasting, acid etching and anodization.

2. Materials and Methods

Four metallic endosteal dental implants with different thread geometries and surface treatments were studied in this paper. The samples are described in Table 1:

Table 1

Samples description

No.	Aspect	Description	Thread shape	Surface treatment
1	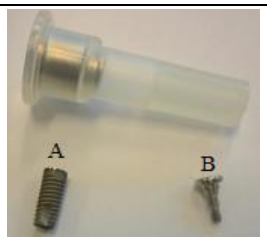	Rootform implant with separate fixture and abutment Ø 3.8 × 10 mm	Square	Machining (mechanical treatment)
2		Rootform implant Ø 5 × 62 mm	V-thread	Abrasive blasting (mechanical treatment)
3	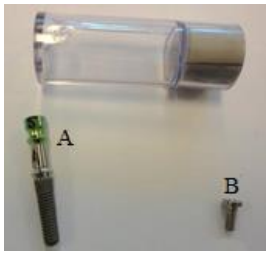	Rootform implant with separate fixture and abutment Ø 3.7 × 13 mm	V-thread	Acid etching (mhemical treatment)

No.	Aspect	Description	Thread shape	Surface treatment
4		Rootform implant Ø 5 × 4,2 × 13 mm	Buttstressed	Anodization (electrochemical treatment)

Radiographic examinations were performed by certified personnel and interpreted by a Level III specialist certified in accordance with SNT-TC-1A. Each sample was analysed using an ERESCO 42 MF3 X-Ray Unit (GE Inspection Technologies) at 120-150 kV and 4.5 mA, with focus-to-film distance of 700 mm, for 3-8 min exposure time. The results were developed on 100 × 240 mm AGFA Structurix D5 X-Ray films.

Material identification of the metallic implants was performed following ASTM E1476 requirements with a portable X-ray fluorescence spectrometer (SPECTRO xSORT Handheld with 4W and 50kV Rh tube).

Morphological evaluation of the dental implants was performed using scanning electron microscopy (SEM). SEM analyses were performed on the dental implants without prior surface preparation. Images were captured on a Phillips XL30 ESEM TMP equipment, at 25 kV acceleration voltage and 10 mm working distance, using a SE detector. The macroscopical geometrical parameters of the dental implants were measured on SEM images using the ImageJ 1.52a software. Image colorization, 3D enhancement and calculation of roughness parameters were performed on the SEM images using the MountainsMap® software (Digital Surf, Besançon, France).

3. Results and Discussion

Radiographic examination of implant body shape

Radiographic examination (RT), also known as “industrial radiography” is a popular non-destructive examination method which uses X-rays or gamma rays for evaluating the internal structure and integrity of a specimen. RT is currently intensively employed for testing and grading of welds in metallic components; other metallic and non-metallic parts are also tested in aerospace, construction or oil and gas industries.

Although extensively used in the industry, RT is used in relatively few research studies on dental implants or related devices. For example, a study on a lot of 300 casted titanium dental frameworks, which was evaluated based on

performance indicators such as the number, location and size or argon inclusions was published in 2002 [16]. Previously, RT examinations were also used for evaluating 150 dental crowns and bridges made out of precious metals. For these products, X-ray exposures revealed various types of imperfections such as occlusal underdimensionings, perforations, retention beads or porosities [9]. Besides quality control, another procedure, which included image acquisition, image capture and digitization, and computer-assisted densitometric image analysis of endosseous titanium implants with sand blasted and acid etched surfaces, was reported for evaluating the dental products after implantation in canine mandibles [17].

In this study, the radiographic examination results, presented in Fig. 1, did not reveal any flaws or defects of the tested parts. This outcome was expected since the dental implants were intended for clinical use so they have been subjected to quality control testing in the final stages of their production.

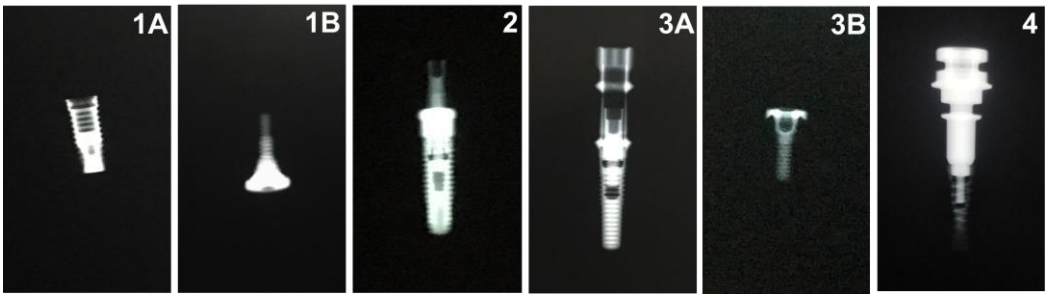

Fig. 1. Radiographic evaluation of the metallic dental implants. For samples 1 and 3, the part marked with A represents the fixture and the part marked with B is the implant's abutment.

Still, the radiographs presented in Fig. 1 have good quality, proving that the method is adequate for evaluating this type of implants. Although the current RT practices for medical devices (such as ASTM F629) refer to casted samples , the reliability and detectability of the radiographic examination of wrought titanium medical devices can be further improved by testing control samples with prefabricated defects or failed dental implants, as well as by comparing the results of this method with a complementary non-destructive testing method [18, 19].

Non-destructive positive material identification

Positive material identification (PMI) using portable X-ray fluorescence spectrometers (XRF) can be performed either directly, by the XRF software which assigns a grade from its library to the compositional results, either by comparing the elemental concentrations provided after the analysis with industry-specific standard material specifications [20, 21]. The second approach was used for the

PMI analysis of the dental materials evaluated in this study; Table 2 presents the elemental concentrations provided by the XRF equipment and the correspondent material specifications.

The PMI results for the fixture and the abutment of the first sample correspond to materials specifications for Cp-Ti (~99% Ti). For the second samples, the XRF equipment identified similar elemental concentrations, except for a higher Al% concentration. However, considering that the surface of the second dental implant was prepared by abrasive blasting with alumina particles, and traces of alumina were previously reported for this type of products, it can be assumed that the second material was manufactured from Cp-Ti. Since the XRF technique was developed for grade identification, a proper discrimination between the purity grades of Cp-Ti is beyond the scope of this method [22-24], however, the standard specification for unalloyed titanium, for surgical implant application (ASTM F67 [25]) is presented in Table 2 as reference.

Table 2

Material identification based on PMI analyses

Sample no. and surface preparation	Component	Ti %	Al %	V %	Si %	Cr %	Ni %	Fe %	Ta %	Sn %
1 machining	A. fixture	99.3	0.22	0.13	0.05	0.02	0.15	0.04	0.05	0.23
	B. abutment	98.7	0.97	0.23	0.06	0.04	0.09	0.03	0.11	0.09
2 abrasive blasting	implant	94.5	4.70	0.09	0.02	0.01	0.20	0.18	0.03	0.16
UNS R50250, UNS R50400, UNS R50550, UNS R50700 acc. to ASTM F67-13(2017) [25]		*Base*	-	-	-	-	-	*Max. 0.20/ 0.50*	-	-
3 acid etching	A. fixture	90.0	5.76	4.34	0.05	0.03	0.19	0.20	0.04	0.19
	B. abutment	90.0	5.91	3.80	0.04	0.05	0.11	0.11	0.06	0.04
4 anodization	implant	88.9	6.92	3.78	0.04	0.04	0.13	0.15	0.05	0.03
UNS R56400 (Ti6Al4V) acc. to ASTM F1472-14[10]		*Base*	*5.50-6.75*	*3.50-4.50*	-	-	-	*Max. 0.30*		-

The PMI analyses of the third and fourth samples identified Al% and V% as main alloying elements, confirming that those dental implants were manufactured from a Ti6Al4V alloy. The results correspond with the standard material specification for wrought Titanium-6Aluminum-4Vanadium alloy for surgical implant applications (ASTM F1472) [10].

Macroscopic evaluation of thread geometry

The thread geometry of a dental implant includes various geometrical parameters such as thread shape, pitch, width, etc. Depending on the patient's biological condition and many local biomechanical factors, these geometrical parameters have different effects on the primary stability, stress concentration and osseointegration of the dental implant [26].

The thread geometries and macrodesign of the dental implants evaluated in this study are presented in the images Fig. 2.1 – 2.4.

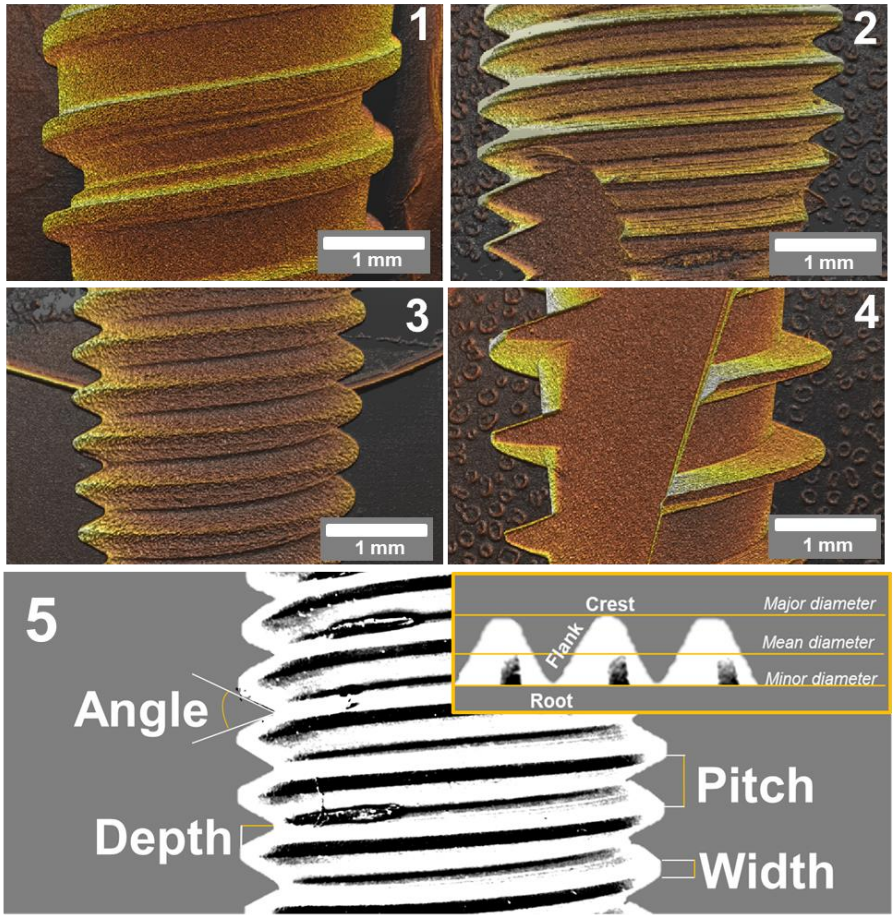

Fig. 2. Macrostructure of dental implants with different thread shapes:
1. square, 2. V-thread, 3. V-thread, 4. buttressed, and 5. schematic representation of the geometrical parameters measured on the macroscopic images using ImageJ software.

These images were digitally processed for measuring several geometrical parameters (which are presented in the schematic representation from Fig. 2.5): pitch, width, depth, flank and angle. The measured values are presented in Table 3.

Thread shape is one of the first geometrical parameter which is taken into account when selecting a dental implant. The macroscopic aspects revealed for the first sample (Fig. 2.1) are characteristic for a square thread, with symmetrical flanks perpendicular to the axis of the screw head, flat crests and relatively high pitches. Different studies suggest that a square thread may provide a better stability in immediate loading [26] (i.e. immediate implant placement after tooth extraction). Grooves were observed in the area between the crests of this implant; these are known to promote osseointegration [26].

The second and third samples (Fig. 2.2 and 2.3) had the aspect of a V-thread, with symmetrical flanks inclined at equal angles, pointed crests, smaller pitches and acute angles between the implant flanks. The fourth sample had the macroscopic aspect of a buttressed implant, with non-symmetrical flanks, and relatively high pitch (Fig. 2.4).

The results obtained after measuring the geometrical implants of the dental implants are presented in Table 3. The implants thread pitch, which is the length measured between two neighbouring threads from the same axis, varied between ~0.50 mm for the V-shaped threads and ~1 mm for the square and buttressed threads. Thread pitch is an important parameter when comparing same length implants, because a smaller pitch is an indication of a higher number of threads, which means a higher surface area to have direct contact with the bone [26].

Table 3

Geometrical parameters measured on the macroscopic images in Fig 2

Sample no. and thread shape	Pitch (mm)	Width (mm)	Depth (mm)	Flank (mm)	Angle (degrees)
1 - Square	1.04 ± 0.02	0.24 ± 0.02	0.23 ± 0.04	0.22 ± 0.05	117 ± 12
2 - V-shape	0.54 ± 0.01	0.13 ± 0.02	0.34 ± 0.01	0.39 ± 0.01	66 ± 4
3 - V-shape	0.53 ± 0.01	0.11 ± 0.01	0.34 ± 0.01	0.41 ± 0.02	61 ± 2
4 - Buttressed	1.13 ± 0.01	0.11 ± 0.01	0.62 ± 0.06	0.52 ± 0.03	113 ± 2

The thread width - the length of the thread crest (the outermost surface joining the two sides of the thread), is closely related to the thread shape and was fairly constant, of ~0.10 mm, for the V-shaped and buttressed threads, and higher (~0.25 mm) for the square thread. Also closely related to thread width, the thread depth (defined as the distance between the outermost tip to the innermost body of the thread [26]) varied between 0.20 – 0.60 mm. Thread width and depth influence the easiness of the surgical procedure (a smaller thread depth will lead to a facile implantation) but are also related to the surface area at the implant-bone interface (higher thread depth and width will provide a higher surface area) [26].

The flank (the side which connects the root with the crest of the thread) and the angle between two neighbouring flanks on the same axis were also

measured. The results varied based on the thread shape, with higher flank values for the V-shaped and buttressed threads, and higher angles for the square and buttressed threads.

Morphological evaluation of implants microdesign

The scanning electron microscopy results for the dental implants are presented in Fig 3. The original SEM images, captured at 500X magnification, are presented in the left column of Fig.3. Illustrative details (different magnifications, suitable chosen to depict the morphological aspects of interest) are also presented in insets for the implant surfaces prepared by abrasive blasting, acid etching and anodization. The digitally processed SEM images are presented in the central column of Fig. 3.

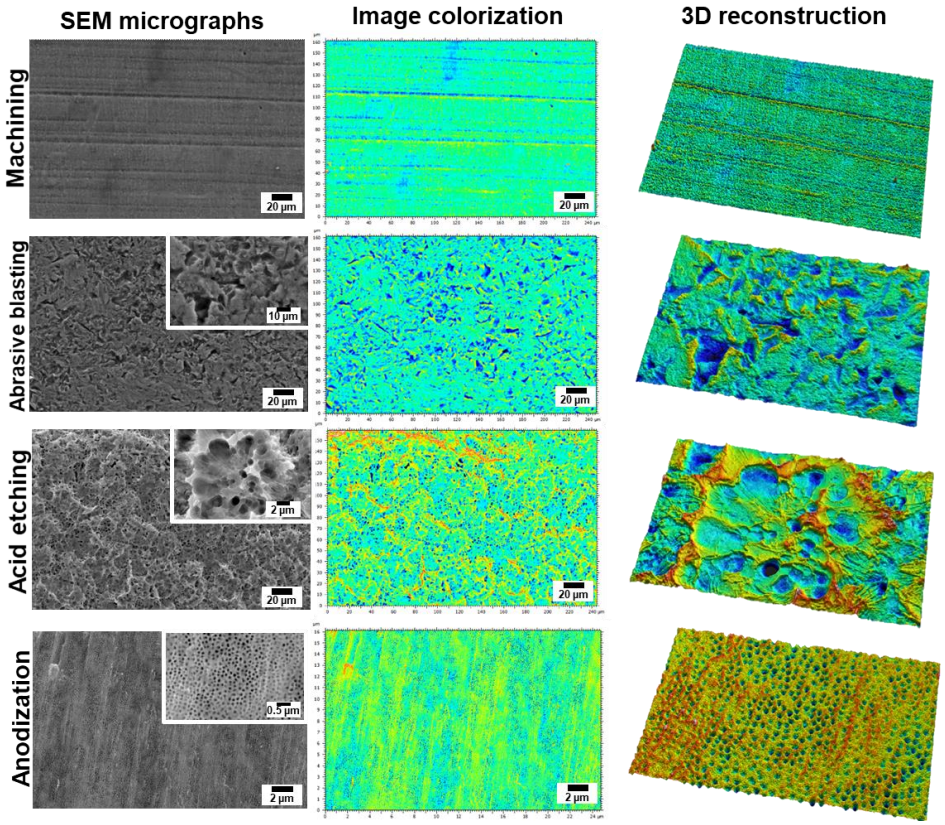

Fig. 3. Morphological evaluation of metallic dental implants. From left to right column: original SEM results, colorized images, and 3D reconstruction of the dental implants surfaces.

In these images, the colour mapping enhanced the topographical features captured by SEM. Surface roughness is visually described by the 3D reconstructed microscopy images (right column, Fig. 3).

The surface of the *machined* titanium implant (Fig. 3) had mainly unidirectional grooves and ridges, remained from the mechanical processing. Three-dimensional reconstruction image showed that the surface of the implant has a relatively low roughness. This is also in agreement with the calculated roughness parameters: R_a= 0.107 μm, R_z= 0.712 μm, R_t= 0.884 μm (presented in Fig. 4).

The *abrasive blasted* implant surface had a heterogeneous area with irregular peaks, cavities with large depths and sharp edges, all resulting from the blasting process (Fig. 3). The surface had a pronounced roughness (R_a= 0.643 μm, R_z=3.82 μm, R_t= 4.25 μm – as presented in Fig. 4). The roughness varies depending on the granulometry of the abrasive media, and this aspect is well emphasized in the image of the three-dimensional reconstruction.

The *acid etching* offered a very complex surface with distinct cavities and no intact areas. Surface texture was characterized by the irregular distribution of the peaks and valleys. Some pits were also observed (Fig. 3). The topographic reconstruction revealed that the estimated distance between the peaks is high, which means that the acid etching does not create a standard topography and leads to a high surface roughness (R_a = 0.26 μm, R_z = 2.01 μm, R_t = 2.57 μm in Fig. 4).

The *anodizing* process modified the crystalline structure of the oxide layer on the surface, which is nanotubular (Fig. 3). TiO_2 nanotubes were formed as a result of the anodization process [27-30]. The nanotubes were grown in a vertically aligned and parallel configuration. The presence of nanotubes offered a low degree of roughness (R_a = 0.0112 μm, R_z = 0.055 μm, R_t = 0.067 μm).

Surface roughness evaluation by microscopic image analysis

Based on the scale of the features, surface roughness can be expressed at macroscopic, microscopic and nanometric levels. In the first level - the macroscopic level (mm – tens of μm) - surface roughness is important for implant fixation and long-term stability of the implants. Macroscopic roughness is related to implant geometry and can be described by means of threaded screws dimensions and by surface treatments results, if these provide a surface roughness of more than 10 μm. At the second roughness level - the microscopical level (1 – 10 μm) - implant roughness is important for facilitating bonding between the metallic implant and the bone [12]. A theoretical estimation reported that the ideal pits for implant bonding have a hemispherical shape with 1.5 μm depth and 4 μm diameter [12]. Finally, at the third roughness level – nanometric level – surface roughness has a role in protein adsorption and bone cells adhesion, thus influencing the osseointegration [12, 31, 32].

The surface roughness of the four dental implants was evaluated by analysing SEM results with a dedicated image analysis software. Starting from the 3D reconstruction of a calibrated SEM image (Fig. 3), the program characterized

the surface roughness and texture, using roughness/waviness filtering techniques. Various amplitude parameters were estimated using the generated roughness profiles, in accordance with ISO 4287 standard (Fig. 4) [33].

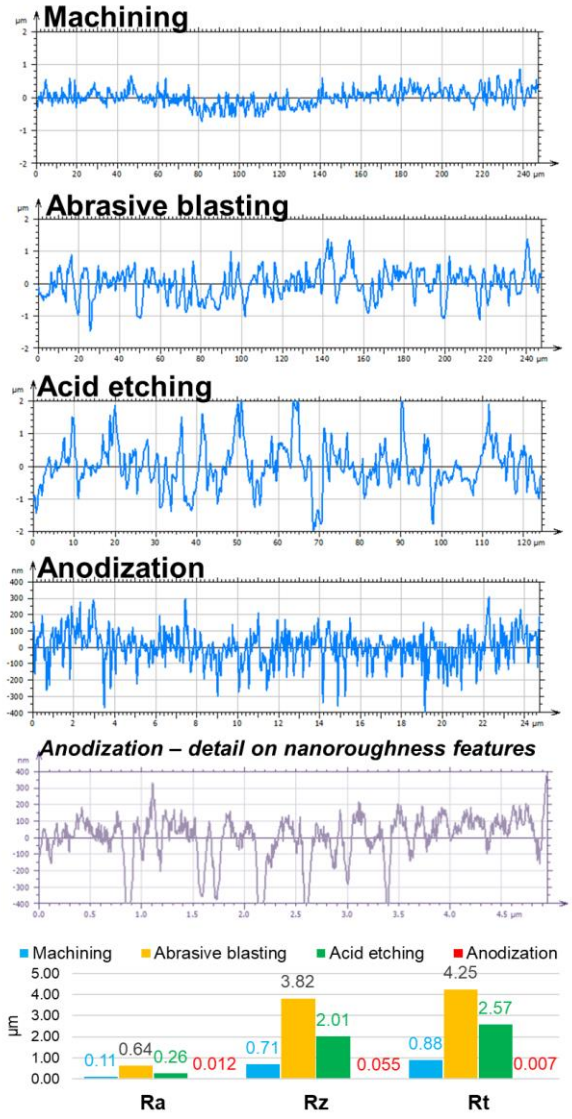

Fig. 4. Roughness profiles generated after SEM image analysis for different surface treatments of titanium dental implants, with a profile detail provided for a better display of the nanoroughness features induced by anodization, and the variation chart for Ra, Rz and Rt parameters

The profiles (Fig. 4) presented for the dental implants with surfaces prepared by machining, abrasive blasting and acid etching were generated based

on a 240 μm evaluation length for machining and abrasive blasting, and a 120 μm evaluation length for acid etching.

By contrast, due to the lower roughness, the profile of the anodized surface is presented for 24 μm evaluation length. A profile detail of the anodized surfaces based on a 4.5 μm evaluation length is also provided in Fig. 4 for a better display of the nanoroughness features.

The results for R_a, R_z and R_t values provided by the software are compared in the bar graph presented in Fig. 4. All values were computed from profiles generated on 240 μm evaluation lengths. Three roughness parameters were evaluated:

- **R_a** represents the arithmetical mean roughness value, which is the arithmetical mean of the absolute values of the profile deviations from the mean line of the roughness profile;
- **R_t** represents the total height of the roughness profile and is calculated as the difference between the height of the highest peak and the depth of the deepest valley in the evaluation length;
- **R_z** represents the mean roughness depth, which is the mean value of the five greatest heights of the roughness profile within the evaluation length.

The highest values for all roughness parameters were obtained for the surface prepared by abrasive blasting, while the lowest values were determined for the anodized surface. The surfaces prepared by machining and acid etching had similar R_a values, but different R_t and R_z values (higher values for acid etching), which confirms that acid etching provided a more rougher implant surface. The results are supported by the morphological aspects of the samples (presented in Fig. 3) from which it can clearly be observed that abrasive blasting and acid etching provided rougher surfaces than machining and anodization.

4. Conclusions

The quality control sequence proposed in this study was suitable for evaluating various material parameters which are essential for the successful application of a dental implant. All parameters – presence of internal defects, material grade, body shape, thread geometry, surface morphology and surface roughness were evaluated in a non-destructive manner. RT examinations displayed no structural, geometrical or compositional deflections. The biomaterials composition was compared to material grades according to ASTM standards for medical devices. Also, the corroboration of experimental methods (SEM) and image processing (Mountains Map, ImageJ) proved very helpful for evaluating the thread geometry and surface roughness of the implants. The quality control sequence is adequate for testing entire batches of dental implants in a reproducible manner and can be further improved by employing more testing

methods (such as portable hardness testing) or by comparing the results with material specifications provided by the manufacturers.

Acknowledgement

The authors wish to acknowledge the contribution of technical personnel of Nuclear NDT Research & Services, Bucharest, Romania, in performing the radiographic examinations and PMI analyses. Also, all authors are thankful to Digital Surf, Besançon, France, for their technical support and for providing the software MountainsMap used in processing of SEM images for evaluating the roughness parameters.

R E F E R E N C E S

1. Grand View Research Inc., Dental Implants Market Size, Share & Trends Analysis Report By Product (Titanium Implants, Zirconium Implants), By Region (North America, Europe, Asia Pacific, Latin America, MEA), And Segment Forecasts, 2018 - 2024, https://www.grandviewresearch.com/industry-analysis/dental-implants-market accessed on 16.12.2018.
2. Miculescu, F., et al., Experimental researches on biomaterial-tissue interface interactions. Journal of Optoelectronics and Advanced Materials, 2007. **9**(11): p. 3303-3306.
3. Miculescu, F., et al., Researches regarding the microanalysis results optimisation on multilayer nanostructures investigations. Digest Journal of Nanomaterials & Biostructures (DJNB), 2011. **6**(2).
4. Marinescu, R., et al., Complications related to biocomposite screw fixation in ACL reconstruction based on clinical experience and retrieval analysis. Materiale Plastice, 2015. **52**(3): p. 340-344.
5. Antoniac, I.V., et al., IOL's Opacification: A Complex Analysis Based on the Clinical Aspects, Biomaterials Used and Surface Characterization of Explanted IOL's. Materiale Plastice, 2015. **52**(1): p. 109-112.
6. Pariza, G., C.I. Mavrodin, and I. Antoniac, Dependency between the porosity and polymeric structure of biomaterials used in hernia surgery and chronic mesh-infection. Materiale Plastice, 2015. **52**(4): p. 484-486.
7. Herø, H., M. Syverud, and M. Waarli, Mold filling and porosity in castings of titanium. Dental materials, 1993. **9**(1): p. 15-18.
8. Dharmar, S., R.J. Rathnasamy, and T. Swaminathan, Radiographic and metallographic evaluation of porosity defects and grain structure of cast chromium cobalt removable partial dentures. Journal of Prosthetic Dentistry, 1993. **69**(4): p. 369-373.
9. Eisenburger, M. and H. Tschernitschek, Radiographic inspection of dental castings. Clinical oral investigations, 1998. **2**(1): p. 11-14.
10. ASTM F1472-14, Standard Specification for Wrought Titanium-6Aluminum-4Vanadium Alloy for Surgical Implant Applications (UNS R56400), ASTM International, West Conshohocken, PA, 2014, www.astm.org.
11. Jemat, A., et al., Surface modifications and their effects on titanium dental implants. BioMed research international, 2015. **2015**.
12. Le Guéhennec, L., et al., Surface treatments of titanium dental implants for rapid osseointegration. Dental materials, 2007. **23**(7): p. 844-854.
13. Maidaniuc, A., et al., Effect of micron sized silver particles concentration on the adhesion induced by sintering and antibacterial properties of hydroxyapatite microcomposites. Journal of Adhesion Science and Technology, 2016. **30**(17): p. 1829-1841.

14. Miculescu, F., et al., Effect of heating process on micro structure level of cortical bone prepared for compositional analysis. Digest Journal of Nanomaterials and Biostructures, 2011. **6**(1): p. 225-233.
15. Earar, K., et al., Etching treatment effect on surface morphology of dental structures. Revista de Chimie, 2017. **68**(11): p. 2700-2703.
16. Cecconi, B.T., et al., Casting titanium partial denture frameworks: a radiographic evaluation. Journal of Prosthetic Dentistry, 2002. **87**(3): p. 277-280.
17. Cochran, D., et al., Evaluation of an endosseous titanium implant with a sandblasted and acid-etched surface in the canine mandible: radiographic results. Clinical Oral Implants Research, 1996. **7**(3): p. 240-252.
18. Miculescu, F., et al., Facile synthesis and characterization of hydroxyapatite particles for high value nanocomposites and biomaterials. Vacuum, 2017. **146**: p. 614-622.
19. Pandele, A., et al., Cellulose acetate membranes functionalized with resveratrol by covalent immobilization for improved osseointegration. Applied Surface Science, 2018. **438**: p. 2-13.
20. Tite, T., et al., Cationic Substitutions in Hydroxyapatite: Current Status of the Derived Biofunctional Effects and Their In Vitro Interrogation Methods. Materials, 2018. **11**(11): p. 2081.
21. Stuart, B.W., J.W. Murray, and D.M. Grant, Two step porosification of biomimetic thin-film hydroxyapatite/alpha-tri calcium phosphate coatings by pulsed electron beam irradiation. Scientific reports, 2018. **8**.
22. Wien, K., et al., Fast application of X-ray fluorescence spectrometry aboard ship: how good is the new portable Spectro Xepos analyser? Geo-Marine Letters, 2005. **25**(4): p. 248-264.
23. Kuncser, V., et al., Magnetic properties of Fe–Co ferromagnetic layers and Fe–Mn/Fe–Co bilayers obtained by thermo-ionic vacuum arc. Journal of Alloys and Compounds, 2010. **499**(1): p. 23-29.
24. Miculescu, F., et al., A study on the influence of the primary electronbeam on nanodimensional layers analysis. Dig. J. Nanomater. Biostruct, 2011. **6**(1): p. 307-317.
25. ASTM F67-13(2017), Standard Specification for Unalloyed Titanium, for Surgical Implant Applications (UNS R50250, UNS R50400, UNS R50550, UNS R50700), ASTM International, West Conshohocken, PA, 2017, www.astm.org.
26. Ryu, H.-S., et al., The influence of thread geometry on implant osseointegration under immediate loading: a literature review. The journal of advanced prosthodontics, 2014. **6**(6): p. 547-554.
27. Duta, L., et al., Comparative physical, chemical and biological assessment of simple and titanium-doped ovine dentine-derived hydroxyapatite coatings fabricated by pulsed laser deposition. Applied Surface Science, 2017. **413**: p. 129-139.
28. Popa, A., et al., Bioglass implant-coating interactions in synthetic physiological fluids with varying degrees of biomimicry. International journal of nanomedicine, 2017. **12**: p. 683.
29. Miculescu, F., et al., Influence of the modulated two-step synthesis of biogenic hydroxyapatite on biomimetic products' surface. Applied Surface Science, 2018. **438**: p. 147-157.
30. Miculescu, F., et al., Cortical bone as resource for producing biomimetic materials for clinical use. Digest J Nanomater Biostruct, 2012. **7**: p. 1667-77.
31. Rupp, F., et al., Surface characteristics of dental implants: A review. Dental Materials, 2018. **34**(1): p. 40-57.
32. Antoniac, I., C. Sinescu, and A. Antoniac, Adhesion aspects in biomaterials and medical devices. Journal of Adhesion Science and Technology, 2016. **30**(16): p. 1711-1715.
33. ISO 4287:1997 - Geometrical Product Specifications (GPS) - Surface texture: Profile method - Terms, definitions and surface texture parameters.